Synthesis, X-Ray Crystallographic Characterization, and Electronic Structure Studies of a Di-Azide Iron(III) Complex: Implications for the Azide Adducts of Iron(III) Superoxide Dismutase

*Laurie E. Grove, Jason K. Hallman, Joseph P. Emerson, Jason A. Halfen, and Thomas C. Brunold**

Supporting Information.

Table S1. Crystal structure coordinates for $LFe(N_3)_2$ measured in Å used for geometry optimization input files.

Table S2. Cartesian coordinates (Å) for a DFT energy minimized model of $LFe(N_3)_2$ using the BP functional.

Table S3. Cartesian coordinates (Å) for a DFT energy minimized model of $LFe(N_3)_2$ using the B3LYP functional.

Table S4. Zero-field splitting parameters from INDO/S-CI calculations for all models of $LFe(N_3)_2$.

Table S5. ORCA DFT (B3LYP) calculated spin-down molecular orbital energies (eV), occupancies, and compositions (%) for the $LFe(N_3)_2$ model derived from the crystal structure.

Table S6. ORCA DFT (PBE0) calculated spin-down molecular orbital energies (eV), occupancies, and compositions (%) for the ORCA (BP) geometry optimized $LFe(N_3)_2$ model.

Table S7. ORCA DFT (PBE0) calculated spin-down molecular orbital energies (eV), occupancies, and compositions (%) for the ORCA (B3LYP) geometry optimized $LFe(N_3)_2$ model.

Table S8. Experimental transitions energies (cm^{-1}) and TD-DFT predicted transition energies (cm^{-1}) and band assignments using the B3LYP functional and the $LFe(N_3)_2$ model derived from the crystal structure coordinates.

Table S9. Experimental transitions energies (cm^{-1}) and TD-DFT predicted transition energies (cm^{-1}) and band assignments using the PBE0 functional and the $LFe(N_3)_2$ model geometry optimized using the BP functional.

Figure S1. Electronic absorption spectrum of $LFe(N_3)_2$ at room temperature.

Figure S2. Electronic absorption and variable temperature MCD spectra collected at 4.5 K of a $LFe(N_3)_2$ mull sample.

Figure S3. Contour plot of χ^2 values as a function of D and E/D parameters for fits of VTVH MCD data collected for $LFe(N_3)_2$ at 20 661 cm^{-1} (484 cm^{-1}). Transition polarizations are given in Table S10.

Table S10. Zero-field splitting parameters D (cm^{-1}) and E/D, polarizations (%) and χ^2 values from an analysis of VTVH MCD data for $LFe(N_3)_2$ collected at 20 661 cm^{-1} (484 nm).

Figure S4. Computed electronic absorption spectrum of $LFe(N_3)_2$ using the B3LYP functional and the model derived from crystal structure coordinates.

Table S1. Crystal structure coordinates for $LFe(N_3)_2$ measured in Å used for geometry optimization input files.

Atom	x	y	z
C	2.550873	1.961853	-0.016510
C	2.902771	1.576569	-1.564438
O	0.503525	-2.187622	-3.339844
N	1.184326	-1.873810	0.142288
N	2.007782	0.756241	0.761063
N	-0.218826	-0.493561	2.177048
C	2.605148	-1.503342	-0.086716
C	3.005905	-0.343704	0.808900
C	1.626083	1.192932	2.127213
C	0.938293	0.100143	2.920959
C	-0.181137	-1.975769	2.203049
C	1.008179	-2.548325	1.455414
C	0.697189	-2.647507	-1.009491
C	0.512238	-1.735840	-2.206436
C	3.820847	2.727325	0.761734
O	0.374298	-0.491364	-1.912231
C	-1.548309	-0.018768	2.777481
C	-1.827423	-0.616043	4.156204
C	-1.676804	1.472458	2.810577
H	1.766052	2.750977	-0.001343
H	3.293518	2.470596	-2.099900
H	1.987610	1.214127	-2.083984
H	3.672607	0.773132	-1.591171
H	2.731705	-1.208435	-1.152374
H	3.246552	-2.384262	0.139603
H	3.066162	-0.690613	1.850983
H	3.978714	0.071777	0.462891
H	0.938370	2.061554	2.020950
H	2.557556	1.501328	2.652542
H	1.662064	-0.720566	3.124420
H	0.542908	0.525635	3.870407
H	-1.122711	-2.342728	1.736649
H	-0.134125	-2.290680	3.269531
H	1.930800	-2.401871	2.060532
H	0.847107	-3.635727	1.281464
H	-0.285568	-3.099747	-0.748000
H	1.451508	-3.425232	-1.264130
H	3.534683	2.969238	1.809814
H	4.080322	3.670074	0.230225
H	4.714737	2.064392	0.774048
H	-2.358353	-0.316650	2.074844
H	-2.800354	-0.239838	4.544205
H	-1.019226	-0.329636	4.865800
H	-1.869095	-1.726120	4.088638
H	-2.656174	1.760406	3.254059
H	-1.611786	1.883194	1.778198
H	-0.858337	1.911621	3.423767
N	-0.518570	1.902191	-0.193329
N	-1.616302	2.220000	-0.607864
N	-2.621246	2.565765	-0.986496
N	-1.832809	-0.774643	-0.186646
N	-2.528351	-0.917221	-1.136703
N	-3.231308	-1.065079	-1.992767
Fe	0.000000	0.000000	0.000000

Table S2. Cartesian coordinates (Å) for DFT energy minimized model of $LFe(N_3)_2$ using the BP functional.

Atom	x	y	z
N	0.800186	-1.790115	-0.122787
N	1.976456	-1.959427	-0.447540
N	3.097076	-2.155624	-0.732910
N	1.594116	1.159821	0.013504
N	2.328918	1.425171	-0.938370
N	3.055161	1.707443	-1.814209
C	-2.227921	-2.464157	-0.002853
C	-2.535339	-2.178818	-1.482224
O	-0.870483	2.030106	-3.382065
N	-1.642014	1.621216	0.122086
N	-1.994446	-1.179900	0.775543
N	-0.044373	0.541061	2.305191
C	-2.942627	0.961502	-0.151245
C	-3.174530	-0.265869	0.745041
C	-1.563339	-1.490524	2.165955
C	-1.113358	-0.261337	2.971329
C	-0.374939	1.998352	2.264038
C	-1.626175	2.325485	1.432037
C	-1.249023	2.471359	-1.031891
C	-0.833237	1.581024	-2.234695
C	-3.295029	-3.377914	0.640518
O	-0.454193	0.356079	-1.896149
C	1.320236	0.351410	2.956879
C	1.422470	1.007294	4.350357
C	1.735382	-1.126663	3.023407
H	-1.251968	-2.981094	0.031372
H	-2.675354	-3.133591	-2.016663
H	-1.713226	-1.629379	-1.968216
H	-3.467773	-1.600876	-1.618408
H	-2.930222	0.645584	-1.205688
H	-3.785355	1.676773	-0.027847
H	-3.416443	0.053955	1.772858
H	-4.077606	-0.789230	0.383972
H	-0.730225	-2.209274	2.080215
H	-2.371689	-1.978195	2.751419
H	-1.978455	0.389847	3.179214
H	-0.779358	-0.618546	3.962173
H	0.505600	2.502365	1.830231
H	-0.538818	2.409195	3.281250
H	-2.536575	2.050110	1.992020
H	-1.679657	3.422485	1.294861
H	-0.375320	3.080566	-0.742172
H	-2.062653	3.155212	-1.343536
H	-3.056778	-3.627518	1.687897
H	-3.341278	-4.330368	0.087051
H	-4.306854	-2.933792	0.615829
H	2.014511	0.862671	2.265610
H	2.425766	0.813263	4.763611
H	0.686279	0.591980	5.062195
H	1.293808	2.101044	4.315735
H	2.741898	-1.195465	3.467590
H	1.771606	-1.584244	2.025040
H	1.062012	-1.730942	3.656906
Fe	0.000000	0.000000	0.000000

Table S3. Cartesian coordinates (Å) for DFT energy minimized model of $LFe(N_3)_2$ using the B3LYP functional.

Atom	x	y	z
N	0.632187	-1.848450	-0.112289
N	1.761871	-2.128922	-0.453339
N	2.829865	-2.417831	-0.752319
N	1.697510	0.991440	-0.023132
N	2.440689	1.176239	-0.963623
N	3.166946	1.375107	-1.826630
C	-2.466156	-2.214722	0.021561
C	-2.755371	-1.900757	-1.450439
O	-0.680237	2.091812	-3.344406
N	-1.468048	1.789688	0.136368
N	-2.097839	-0.971481	0.797684
N	0.034500	0.550568	2.308685
C	-2.816574	1.255356	-0.119812
C	-3.158829	0.061447	0.773010
C	-1.677612	-1.313995	2.172470
C	-1.097504	-0.141800	2.967484
C	-0.148895	2.022705	2.260056
C	-1.361038	2.471268	1.439255
C	-0.999130	2.579285	-1.017197
C	-0.685608	1.650970	-2.218475
C	-3.604507	-3.013184	0.682129
O	-0.437073	0.414261	-1.867523
C	1.374084	0.220245	2.934448
C	1.557526	0.862106	4.318115
C	1.638641	-1.286011	2.999619
H	-1.553741	-2.830109	0.042374
H	-3.008148	-2.832825	-1.984802
H	-1.880951	-1.446823	-1.943970
H	-3.615494	-1.218765	-1.580017
H	-2.853668	0.946457	-1.173203
H	-3.581665	2.048019	0.017197
H	-3.353897	0.406479	1.799545
H	-4.115356	-0.362457	0.426926
H	-0.928497	-2.115829	2.084259
H	-2.523438	-1.710449	2.768509
H	-1.890289	0.589005	3.182587
H	-0.797745	-0.530746	3.954361
H	0.771561	2.439255	1.824158
H	-0.266205	2.446762	3.275833
H	-2.286102	2.290131	2.008500
H	-1.307434	3.567627	1.306534
H	-0.070343	3.103714	-0.737991
H	-1.741989	3.338806	-1.326874
H	-3.374786	-3.272293	1.729172
H	-3.756180	-3.964508	0.144700
H	-4.568359	-2.471268	0.670609
H	2.107422	0.654343	2.237396
H	2.539047	0.572266	4.728668
H	0.785751	0.523254	5.033493
H	1.535034	1.963074	4.280579
H	2.631119	-1.458710	3.448380
H	1.629562	-1.742935	2.001373
H	0.903366	-1.819351	3.627457
Fe	0.000000	0.000000	0.000000

Table S4. Zero-field splitting parameters from INDO/S-CI calculations for all models of $LFe(N_3)_2$.

	Crystal structure	Geometry Optimized Models	
		ORCA (BP)	ORCA (B3LYP)
D (cm^{-1})	-0.341	-0.422	-0.417
E/D	0.228	0.136	0.155

Table S5. ORCA DFT (B3LYP) calculated spin-down molecular orbital compositions and energies for the model derived from the crystal structure.

			Fe d-orbitals					$Azide_1$	$Azide_2$	Carboxylate
MO	E (eV)	occ	xy	yz	xz	x^2-y^2	z^2	p-orbitals[1]	p-orbitals[1]	p-orbitals[1]
100	-7.2220	1	1	0	6	0	0	0	5	39
101	-6.7557	1	6	0	0	0	1	37	10	0
102	-6.3291	1	1	5	0	1	1	27	1	33
103	-6.2453	1	0	3	0	5	0	12	20	23
104	-6.2108	1	2	1	2	0	1	5	26	22
105	-5.9533	1	1	1	0	5	1	16	34	3
106	-2.7522	0	37	9	1	31	0	2	4	0
107	-2.6692	0	2	59	9	12	0	2	2	1
108	-2.6392	0	1	8	69	0	8	1	1	1
109	-1.5841	0	17	0	4	17	28	1	3	1
110	-1.5124	0	16	1	1	13	37	2	0	1

Table S6. ORCA DFT (PBE0) calculated spin-down molecular orbital energies (eV), occupancies, and compositions (%) for the ORCA (BP) geometry optimized $LFe(N_3)_2$ model.

			Fe d-orbitals					$Azide_1$	$Azide_2$	Carboxylate
MO	E	occ	xy	yz	xz	x^2-y^2	z^2	p-orbitals[1]	p-orbitals[1]	p-orbitals[1]
100	-7.8499	1	1	0	5	0	0	1	10	38
101	-7.2828	1	4	0	0	2	1	64	20	0
102	-6.9750	1	0	2	0	0	1	14	0	5
103	-6.9475	1	4	0	0	2	1	4	51	4
104	-6.8720	1	0	4	1	4	0	48	15	4
105	-6.5494	1	0	2	0	4	0	31	31	3
106	-2.7551	0	5	39	1	31	1	11	3	2
107	-2.6622	0	5	39	0	37	0	5	4	1
108	-2.5522	0	0	1	81	1	5	1	3	2
109	-2.0305	0	50	0	0	7	6	10	16	1
110	-1.8502	0	6	0	3	1	60	9	2	5

Table S7. ORCA DFT (PBE0) calculated spin-down molecular orbital energies (eV), occupancies, and compositions (%) for the ORCA (B3LYP) geometry optimized $LFe(N_3)_2$ model.

			Fe d-orbitals					$Azide_1$	$Azide_2$	Carboxylate
MO	E	occ	xy	yz	xz	x^2-y^2	z^2	p-orbitals[1]	p-orbitals[1]	p-orbitals[1]
100	-7.8499	1	1	0	6	0	0	1	10	38
101	-7.2828	1	5	0	0	1	1	62	20	0
102	-6.9750	1	0	1	0	0	1	11	1	5
103	-6.9475	1	3	1	0	3	1	6	50	4
104	-6.8720	1	1	5	1	3	0	50	14	5
105	-6.5494	1	0	2	0	4	0	29	33	3
106	-2.7551	0	12	37	0	28	1	10	3	1
107	-2.6622	0	11	41	1	29	0	4	4	1
108	-2.5522	0	0	0	81	0	6	2	2	3
109	-2.0305	0	42	0	0	16	5	10	10	1
110	-1.8502	0	4	1	4	2	61	8	1	5

Table S8. Experimental transitions energies (cm^{-1}) and TD-DFT predicted transition energies (cm^{-1}) and band assignments using the B3LYP functional and the $LFe(N_3)_2$ model derived from the crystal structure coordinates.

Transition	Experimental	Calculated[2]	Peak Assignments[3]
1	15 200	15 441	$azide_2\ \pi^{nb}(op) \rightarrow 106\text{-}108$
		15 913	$azide_2\ \pi^{nb}(op) \rightarrow 106\text{-}108$
		16 031	$azide_2\ \pi^{nb}(op) \rightarrow 107/108$
2	17 300	16 289	$azide_2\ \pi^{nb}(ip) \rightarrow 106\text{-}108$
		17 291	$azide_2\ \pi^{nb}(ip) \rightarrow 106\text{-}108$
3	19 100	18 523	$azide_2\ \pi^{nb}(ip) \rightarrow 107$
		18 906	$azide_2\ \pi^{nb}(ip) \rightarrow 108$
4	20 650	19 772	$azide_1\ \pi^{nb}(op) \rightarrow 106\text{-}108$
		21 167	$azide_1\ \pi^{nb}(ip) \rightarrow 106\text{-}108$
		21 635	$azide_1\ \pi^{nb}(op) \rightarrow 107/108$
5	22 500	22 138	$azide_1\ \pi^{nb}(ip) \rightarrow 106$
		22 443	$azide_1\ \pi^{nb}(ip) \rightarrow 107$
		22 734	$azide_1\ \pi^{nb}(ip) \rightarrow 108$
6	24 700	24 110	$azide_2\ \pi^{nb}(op) \rightarrow 109$
		25 808	$azide_2\ \pi^{nb}(op) \rightarrow 110$
		26 376	$azide_1\ \pi^{nb}(op)/azide_2\ \pi^{nb}(op) \rightarrow 109/110$
7	27 150	26 737	$O \rightarrow Fe^{3+}\ 3d$
		27 080	$O \rightarrow Fe^{3+}\ 3d$
		27 820	$O \rightarrow Fe^{3+}\ 3d$
		28 324	$O \rightarrow Fe^{3+}\ 3d$
		29 277	$O \rightarrow Fe^{3+}\ 3d$
8	29 100	30 697	$azide_2\ \pi^{nb}(ip) \rightarrow 109$
9	31 130	31 472	$azide_1\ \pi^{nb}(op) \rightarrow 109$
		31 856	$azide_1\ \pi^{nb}(ip) \rightarrow 109$
		32 440	$azide_1\ \pi^{nb}(ip) \rightarrow 110$
10	33 600	32 935	$O \rightarrow Fe^{3+}\ 3d$

Table S9. Experimental transitions energies (cm^{-1}) and TD-DFT predicted transition energies (cm^{-1}) and band assignments using the PBE0 functional and the $LFe(N_3)_2$ model geometry optimized using the BP functional.

Transition	Experimental	Calculated[2]	Peak Assignments[3]
1	15 200		
2	17 300	18 430	$azide_2\ \pi^{nb}(op) \rightarrow 106$
		18 941	$azide_2\ \pi^{nb}(op) \rightarrow 107$
3	19 100	19430	$azide_2\ \pi^{nb}(op) \rightarrow 108$
4	20 650	19 907	$azide_2\ \pi^{nb}(ip) \rightarrow 107$
		20 944	$azide_2\ \pi^{nb}(ip) \rightarrow 108$
5	22 500	21 483	$azide_1\ \pi^{nb}(op) \rightarrow 107$
		21 913	$azide_1\ \pi^{nb}(op) \rightarrow 108$
6	24 700	24 362	$azide_1\ \pi^{nb}(ip) \rightarrow 107$
7	27 150	27 042	$azide_2\ \pi^{nb}(op) \rightarrow 110$
		27 617	$azide_2\ \pi^{nb}(ip) \rightarrow 110$
8	29 100	29 390	$azide_1\ \pi^{nb}(op) \rightarrow 110$
		29 790	$O \rightarrow Fe^{3+}\ 3d$
9	31 130	31 160	$azide_1\ \pi^{nb}(ip) \rightarrow 110$
		31 333	$O \rightarrow Fe^{3+}\ 3d$
10	33 600	33 029	$O \rightarrow Fe^{3+}\ 3d$

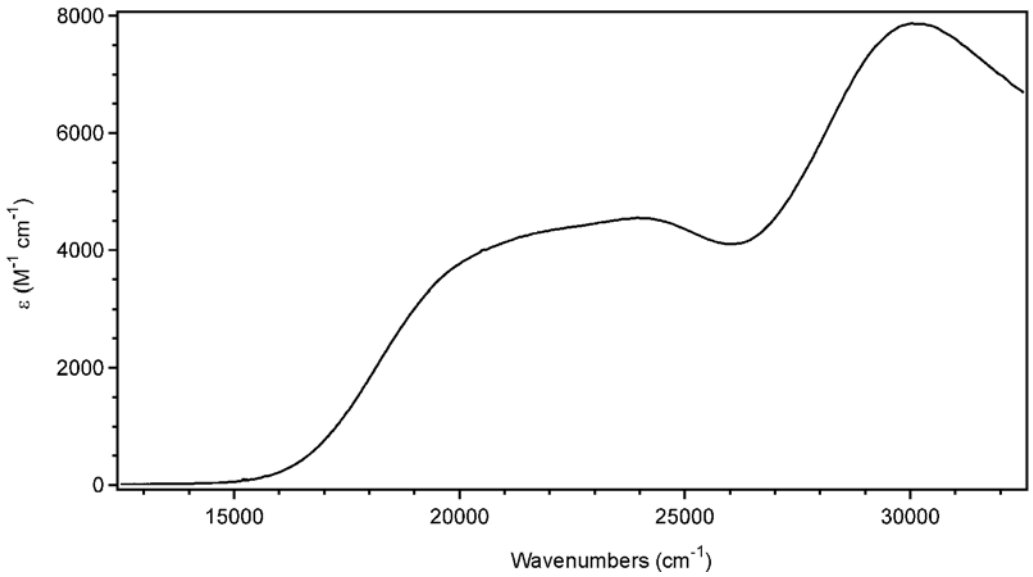

Figure S1. Electronic absorption spectrum of $LFe(N_3)_2$ at room temperature.

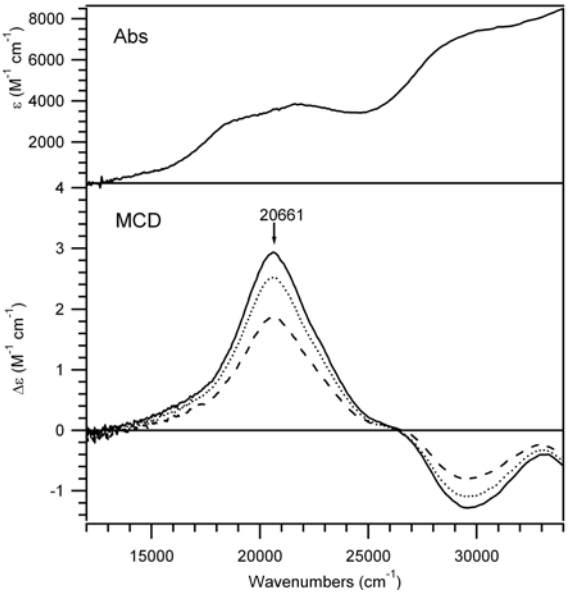

Figure S2. Electronic absorption spectrum at 4.5 K (top) and variable-temperature MCD spectra (4.5, 8, and 15 K) (bottom) of a mull sample of $LFe(N_3)_2$. All MCD features decrease with increasing temperature, consistent with their expected C-term behvaior.

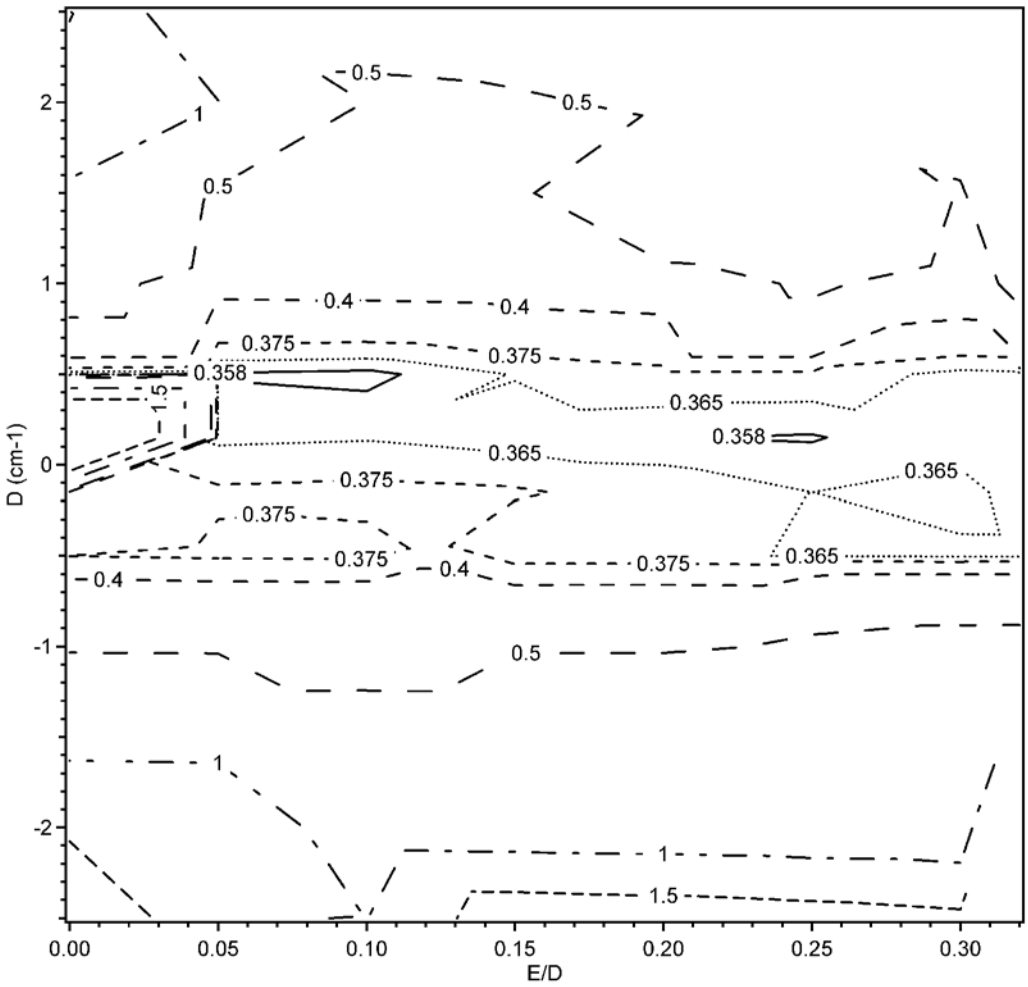

Figure S3. Contour plot of χ^2 values as a function of D and E/D parameters for fits of VTVH MCD data of $LFe(N_3)_2$ collected at 20 661 cm^{-1} (484 nm). Transition polarizations are given in Table S10.

Table S10. Zero-field splitting parameters D (cm^{-1}) and E/D, polarizations (%) and χ^2 values from an analysis of VTVH MCD data for $LFe(N_3)_2$ collected at 20 661 cm^{-1} (484 nm).

D	E/D	x	y	z	χ^2
2.5	0	18	5	77	1.511
2.5	0.05	1	99	0	0.515
2.5	0.1	12	86	1	0.516
2.5	0.15	64	34	2	0.526
2.5	0.2	96	3	0	0.552
2.5	0.25	100	0	0	0.601
2.5	0.3	100	0	0	0.677
2	0	96	1	3	1.397
2	0.05	95	2	3	1.011
2	0.1	0	99	0	0.492
2	0.15	15	84	1	0.495
2	0.2	73	26	1	0.507
2	0.25	98	2	0	0.531
2	0.3	14	72	14	0.571
1.5	0	100	0	0	0.924
1.5	0.05	1	99	0	0.459
1.5	0.1	3	96	1	0.459
1.5	0.15	2	97	0	0.460
1.5	0.2	94	2	4	0.771
1.5	0.25	92	3	6	0.803
1.5	0.3	94	6	0	0.488
1	0	45	28	27	0.584
1	0.05	4	94	2	0.409
1	0.1	14	81	5	0.410
1	0.15	28	67	5	0.412
1	0.2	39	57	4	0.415
1	0.25	100	0	0	0.524
1	0.3	35	64	1	0.425
0.5	0	89	0	10	0.359
0.5	0.05	35	4	60	0.357
0.5	0.1	45	15	41	0.356
0.5	0.15	94	0	6	0.366
0.5	0.2	93	0	7	0.371
0.5	0.25	98	0	2	0.371
0.5	0.3	69	4	27	0.362
0.15	0	6	1	92	3.241
0.15	0.05	13	14	72	0.363
0.15	0.1	6	4	91	0.364
0.15	0.15	45	5	51	0.360
0.15	0.2	68	4	27	0.360
0.15	0.25	90	2	8	0.357
0.15	0.3	62	5	33	0.361

D	E/D	x	y	z	χ^2
-0.15	0	5	3	92	0.389
-0.15	0.05	7	3	90	0.377
-0.15	0.1	49	6	45	0.378
-0.15	0.15	75	4	21	0.376
-0.15	0.2	48	6	46	0.370
-0.15	0.25	28	5	67	0.365
-0.15	0.3	82	3	15	0.368
-0.5	0	10	19	71	0.375
-0.5	0.05	27	7	66	0.372
-0.5	0.1	20	9	71	0.371
-0.5	0.15	33	4	63	0.366
-0.5	0.2	23	6	71	0.366
-0.5	0.25	22	6	72	0.365
-0.5	0.3	23	5	72	0.364
-1	0	1	2	97	0.473
-1	0.05	1	1	98	0.471
-1	0.1	1	1	98	0.472
-1	0.15	0	1	99	0.471
-1	0.2	0	0	99	0.472
-1	0.25	2	1	97	0.520
-1	0.3	1	0	98	0.541
-1.5	0	18	7	75	0.860
-1.5	0.05	7	16	77	0.846
-1.5	0.1	0	0	100	0.530
-1.5	0.15	8	11	80	0.837
-1.5	0.2	11	8	81	0.867
-1.5	0.25	9	8	83	0.852
-1.5	0.3	0	0	100	0.507
-2	0	15	19	65	1.391
-2	0.05	16	18	66	1.382
-2	0.1	0	0	100	0.721
-2	0.15	0	0	100	0.701
-2	0.2	0%	0	100	0.677
-2	0.25	0	0	100	0.650
-2	0.3	0	0	100	0.624
-2.5	0	14	12	74	2.105
-2.5	0.05	0	0	100	1.022
-2.5	0.1	0	0	100	0.993
-2.5	0.15	19	20	60	1.824
-2.5	0.2	20	18	62	1.772
-2.5	0.25	18	18	64	1.695
-2.5	0.3	16	20	64	1.594

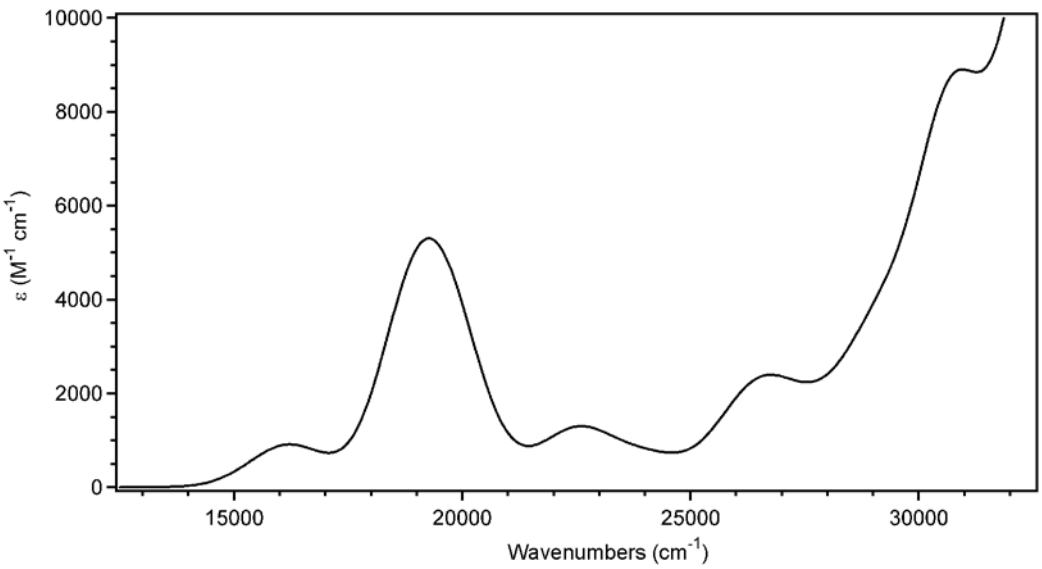

Figure S4. Computed electronic absorption spectrum of $LFe(N_3)_2$ using the B3LYP functional and the model derived from crystal structure coordinates.